DNA-BASED NANOPARTICLES: A PLATFORM TO PROVIDE HIGH ENCAPSULATION, STABILITY AND PROLONGED RELEASE FOR DOXORUBICIN

MARÍA GABRIELA VILLAMIZAR-SARMIENTO [1,2,3], ESTEFANÍA ELGUETA-BRAVO [2,4], ANDREW F. G. QUEST [4,5], FELIPE A. OYARZÚN-AMPUERO [2,3,5], MAURICIO BÁEZ [1*] AND IGNACIO MORENO-VILLOSLADA [6*]*

[1]*Departamento de Bioquímica y Biología Molecular, Facultad de Ciencias Químicas y Farmacéuticas, Universidad de Chile, Santiago, Chile; magabrielavillamizarsarmiento@gmail.com, mauricio.baez@ciq.uchile.cl*
[2]*Department of Sciences and Pharmaceutical Technology, University of Chile, Santiago de Chile 8380494, Chile; estefania.elgueta@uchile.cl, foyarzuna@ciq.uchile.cl*
[3]*Center for New Drugs for Hypertension (CENDHY), Universidad de Chile & Pontificia Universidad Católica de Chile, Santiago, Chile*
[4]*Laboratory of Cellular Communication, Program of Cell and Molecular Biology, Institute of Biomedical Sciences (ICBM), Faculty of Medicine, University of Chile, Av. Independencia 1027, Santiago 8380453, Chile; aquest@u.uchile.cl*
[5]*Advanced Center for Chronic Diseases (ACCDiS), Santiago 8380494, Chile*
[6]*Instituto de Ciencias Químicas, Facultad de Ciencias, Universidad Austral de Chile, Casilla 567, Valdivia 5110033, Chile, imorenovilloslada@uach.cl.*

ABSTRACT

Doxorubicin (DOX) is a potent drug for cancer treatment but presents limitations for encapsulation and prolonged release. Nanoparticles (NPs) are an alternative to mitigate these issues; nevertheless synthetic methods are often complex and inefficient. This study focus in the development of DNA-based NPs, using DNA as unique excipient allowing ionic and aromatic interactions with DOX. **Methods**: The NPs formation consists in the mixture of DNA and DOX in water (aromatic and non-aromatic polyelectrolytes were used as positive and negative controls, respectively). UV-visible and fluorescence spectroscopy were used to corroborate the DOX/DNA interactions and to elucidate the mode of binding. Turbidimetry, dynamic light scattering, laser Doppler anemometry, nanoparticle tracking analyses, ultrafiltration, and scanning transmission electron microcopy were used to characterize the efficiency of the process and the morphology of DOX/DNA NPs. *In vitro* release, viability of non-cancerous cells and stability tests were conducted to assess the release profile and safety of the NPs. **Results**: DOX associates with DNA through ionic and aromatic interactions forming spherical NPs (115-220 nm, polydispersity 0.3-0.5, ~-27 mV, 8-13x10^{11} NPs/mL) with DOX association efficiency of 66-80% and loading in the range of 40-60%. DOX/DNA NPs exhibited prolonged release (55% in 12 days), stability at storage conditions (at least 8 weeks) and does not provide toxicity in non-cancerous cells. **Conclusions:** We provide a simple strategy to entrap and release DOX in the form of NPs in DNA-based platforms. This strategy could be used for other aromatic anticancer drug and selecting DNA sequences able to support anticancer activity.

Keywords: *Nanomedicine; cancer; deoxyribonucleic acid; doxorubicin; aromatic interactions*.

1. INTRODUCTION

Cancer is the second leading cause of morbidity and mortality worldwide, surpassed only by cardiovascular diseases. According to the International Agency for Research on Cancer (IARC) more than 35 million new cases per year are projected to be diagnosed in 2050 [1-4]. This scenario drives the continuous development and optimization of pharmacological therapies, making it a critical area of innovation and research, particularly those aimed at improving the efficacy and safety of existing treatments. Doxorubicin (DOX) is a drug belonging to the anthracycline family and is widely used for the combined chemotherapy of solid tumors, including lung, breast, ovarian, liver, and testicular cancer, among others [5-8]. However, a key challenge in its administration lies in its high cardiotoxicity, as well as its cumulative and irreversible toxicity [9-12]. In addition, DOX is associated with adverse effects such as fatigue, alopecia, nausea, vomiting, oral mucositis, and suppression of bone marrow function, which can increase the risk of infections, anemia, and bleeding. A therapeutic strategy that has gained relevance is the incorporation of DOX into nanoparticles (NPs) [13-18]. These formulations offer superior clinical performance compared to free DOX (a standard treatment), due to improved pharmacokinetics and biodistribution associated with the enhanced permeability and retention (EPR) effect. Moreover, this formulation helps reducing the side effects, especially cardiotoxicity thereby improving therapeutic compliance and patient quality of life. Importantly, some DOX-loaded NPs are FDA-approved (Doxil®, Marqibo®, Onivyde®, Vyxeos®), and many more are in various stages of clinical trials [19]. DOX, is a hydrophilic low molecular-weight drug (579.9 Da), with an amino functional group (pKa: 8.2) and one tetracyclic aromatic ring (**Figure 1**). Currently, research has focused on exploring NPs systems that efficiently entrap and control the release of DOX. However, due to the high water solubility and low molecular-weight, DOX may exhibit weak interactions with many conventional drug carriers, commonly reflecting low association parameters and lack of controlled release, thus limiting its therapeutic application [20-22].

Aromatic interactions refer to intimate non-covalent interactions between aromatic rings containing π-orbitals. They have been used to successfully obtain NPs with high association parameters (association efficiency ≥ 90 % and around 50 % of drug loading) and prolonged drug release profiles [23-25] when hydrophilic, aromatic, and low molecular-weight (HALMW) drugs were combined with a non-biodegradable aromatic polyelectrolyte as unique excipient such as poly(sodium 4-styrenesulfonate) (PSS). This approach has been effective when the following conditions are satisfied: **i)** the drug and the polyelectrolyte exhibited oppositely charged functional groups, **ii)** the presence of aromatic groups in both components, and **iii)** the establishment of intimate contact between these molecules.

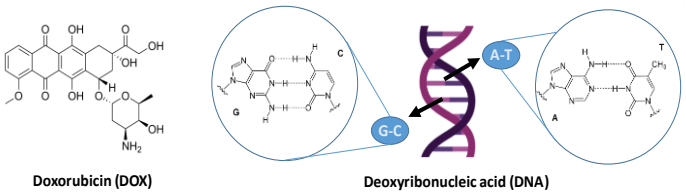

Figure 1.- Molecular structure of doxorubicin and deoxyribonucleic acid (DNA).

The strategy of elaboration is simple and consists in the mixture of two aqueous solutions (one containing the HALMW drug and other containing the PSS) under stirring at room temperature. Importantly, similar formulations using the anionic non-aromatic poly(sodium vinylsulfonate) (PVS) were not able to form NPs with the HALMW drugs, demonstrating the critical role of the aromatic groups in the polyelectrolyte for the NPs formation [23-25]. Furthermore, the obtained NPs demonstrated to be stable at different biological and storage conditions (ionic strength, pH, temperature, and prolonged time) and prolonged release profiles.

Deoxyribonucleic acid (DNA) represents a polyelectrolyte composed of four different monomers (adenine: A, guanine: G, cytosine: C, and thymine: T, **Figure 1**), whose bases engage in aromatic interactions between adjacent nucleotides. The phosphate group within DNA confers a strong polyanionic character to this biological macromolecule [26-28]. Several DNA-based NPs for drug delivery have been reported in the literature [26, 27]. Some of them rely on self-assembly (origami [29, 30] and hydrogels [31]) while others use inorganic materials where DNA acts as a coating (e.g., gold nanoparticles [32]).

**Corresponding author email: mauricio.baez@ciq.uchile.cl (M.B), imorenovilloslada@uach.cl (I.M-V), foyarzuna@ciq.uchile.cl (F.A.O-A)*

Most of the proposed synthesis methods are complex and involve multiple meticulous steps, including temperature shifts (to control hybridization), use of alternative solvents, additional excipients, and even a prior computational design. As a result of these methodologies, which usually require multiple purification processes (e.g., electrophoresis, precipitation, ultrafiltration), these proposals often yield suboptimal output [26, 28]. Interestingly, from a chemical perspective, DNA shares similar characteristics with the polyelectrolyte PSS (both are aromatic and negatively charged), but offers the advantage of being biodegradable and biocompatible. Furthermore, through technologies readily available in laboratories (chemical synthesis and amplification methods such as polymerase chain reaction, PCR), it is possible to precisely define the monomer sequence and the length of the DNA (number of base pairs, bp). In addition, nucleotide-based drugs have been widely proposed and used for cancer therapy (antisense oligonucleotides (ASO) [33-35], small interfering RNA (siRNA) [36, 37], messenger RNA (mRNA) [38-40], and microRNA (miRNAs) [41-43], thus potentially conferring a dual biological activity if they are combined with conventional anticancer drugs.

Due to DOX is also a HALMW drug, in this work we generated DOX/DNA NPs, comprising only two molecules (DOX and DNA), following a simple strategy, and showing high encapsulation, stability and prolonged release profile. This strategy relies on the formation of electrostatic interactions between DOX and DNA stabilized by short-range aromatic interactions. These results could be used as a foundation for the development of novel cancer therapies based in nucleotides-drug interactions.

2. MATERIALS AND METHODS

2.1 Chemicals and Reagents

Doxorubicin hydrochloride (DOX, 579.9 g/mol) was purchased from AK Scientific (California, USA) and was used as received. Deoxyribonucleic acid (DNA, Merck Millipore, Calf Thymus DNA, > 10 kbp, cat. No.: 2618, Germany) was dissolved in water (1 mg/mL) and dialyzed using a Pur-A-Lyzer™ Maxi Dialysis Kit (molecular weight cut-off, MWCO, of 6000 Da, Sigma Aldrich, USA) for 24 h at room temperature, under gentle agitation (Milli-Q water was in the receptor medium). The anionic aromatic polyelectrolyte PSS (206.2 g/mol of monomeric units) was purchased from Sigma Aldrich (USA) and purified/fractionated by diafiltration over a membrane with a MWCO of 5000 Da (Biomax, 63.5 mm diameter), first in the presence of 0.15 M $NaNO_3$ (Sigma Aldrich, USA) and then in the absence of the electrolyte. The anionic aliphatic polyelectrolyte PVS (130.1 g/mol of monomeric units) was purchased from Sigma Aldrich (USA) and was used as received. The pH of DOX solution was adjusted with an Edge® HI2002 pH meter (Hanna Instruments, USA) with minimum amounts of NaOH and HCl (Merck, Germany). All the solutions were prepared with Milli-Q water obtained from a Simplicity SIMS 00001 equipment (Millipore, France). Media used for cell assays, including antibiotics (RPMI 1640, DMEM high glucose, penicillin and streptomycin) were from Gibco-BRL(UK); fetal bovine serum (FBS) was from Hyclone (Cytiva, US); the 3-(4,5-dimetylthiazol-2-yl)-5-(3-carboxymethoxyphenil)-2-(4-sulfophenyl)-2H-tetrazolium inner salt (MTS) proliferation assay kit was from Promega (US).

2.2 UV-vis absorption spectra

The UV-vis spectra were acquired with a Duetta spectrophotometer (Horiba Scientific, Japan) using a quartz cuvette (Hellman®, Germany) of 1 cm of path length. Equal volumes (500 µL each) of DOX and DNA were mixed and incubated for 5 minutes at room temperature. For these experiments the DOX concentration was maintained constant (meanwhile varying the DNA concentration) in order to minimize possible concentration - dependent or self - aggregation effects of DOX, which could comprise the accuracy of the measurements. DOX concentration was fixed at 3.5 x 10^{-5} M, while varying the DNA concentration from 0 to 2.5 x 10^{-4} M (the concentration was calculated considering the nucleotides as the monomeric units). The absorption spectra (λ = 200 - 800 nm) were recorded and plotted to illustrate spectroscopic features such as hypochromic and bathochromic shifts. These effects became more pronounced with increasing DNA concentrations and provide qualitative insight into DOX-DNA interactions. To determine intrinsic binding constant, K_b, the concentration of DOX was fixed at 3.5 x 10^{-5} M, while the concentration of DNA was varied between 1 x 10^{-6} M to 2.5 x 10^{-5} M. Absorbance values at 495 nm (the characteristic wavelength of DOX) were recorded and fitted to equation (1), derived from the classical binding model described by Wolfe-Shimer for drug-DNA interactions [44-50]:

$$\frac{[\mathrm{DNA}]}{(\varepsilon_a - \varepsilon_f)} = \frac{1}{K_b(\varepsilon_{b-}\varepsilon_f)} + \frac{1}{(\varepsilon_b - \varepsilon_f)}[DNA] \qquad \text{equation (1)}$$

where ε_a, ε_f, and ε_b represent the molar absorption coefficients associated with the interaction between DOX and DNA. Specifically, ε_f is the extinction coefficient of free DOX in solution, determined from a calibration curve obtained in the absence of DOX. This curve was experimentally established over a DOX concentration range of 1×10^{-5} M to 9×10^{-5} M, yielding a molar extinction coefficient of 9261.6 $M^{-1}\cdot cm^{-1}$. ε_a is the apparent extinction coefficient of DOX at a given DNA concentration and is calculated as the ratio of the observed absorbance to the concentration of DOX (A_{obs}/[DOX]). ε_b corresponds to the extinction coefficient of DOX when it is fully bound to DNA. [DNA]/(ε_a-ε_f) reflects the change in DOX absorbance due to partial binding of DOX to DNA at varying DNA concentrations. [DNA]/(ε_b-ε_f) represents the scenario where DOX is fully bound to DNA, indicating the maximum binding site saturation. A plot of [DNA]/(ε_a-ε_f) versus [DNA] yielded a straight line, where the slope m and y-intercept b where used to calculate the intrinsic binding constant K_b as

$$K_b = \frac{m}{b} \qquad \text{equation (2)}$$

2.3 Fluorescence spectroscopy

All fluorescence spectra were recorded on Duetta spectrophotometer (Horiba Scientific, Japan) using a quartz cuvette (Hellman®, Germany) of 1 cm of path length. Equal volumes (500 µL each) of DOX and DNA were mixed and incubated for 5 min at room temperature. DOX concentration was fixed at 3.5 x 10^{-5} M, while varying the DNA concentration from 0 to 2.5 x 10^{-4} M, in terms of nucleotides. The excitation wavelength was set to 480 nm, and emission was collected at 590 nm with a bandwidth of 10 nm. The intensity values at λ = 590 nm (characteristic wavelength of DOX) at the tested DOX concentration were fitted to equation (2) to obtain the Stern-Volmer quenching constant, K_{sv} [49]:

$$\frac{F_0}{F} = 1 + K_{sv}[Q] \qquad \text{equation (3)}$$

where F_0 and F denote the steady-state fluorescence intensities in the absence and in the presence of the quencher, respectively, K_{sv} is the Stern–Volmer quenching constant, and [Q] is the concentration of the DNA.

2.4 Preparation and physicochemical characterization of DOX/DNA NPs

DOX/DNA formulations were synthetized according to the method previously reported by our group [23-25]. Briefly, 500 µL of an aqueous solution containing the cationic DOX was added to 500 µL of an aqueous solution containing the anionic DNA, both at pH 7 (adjusted with minimum amounts of HCl 0.1 M and NaOH 0.1 M) and exposed to continuous stirring for 5 min. In all formulations the concentration of DNA was constant (1.44 x 10^{-3} nucleotides/L), while the concentration of the DOX was selected to obtain final molar ratio ranging between 0.1 and 1.0 (1.44 x 10^{-4} - 1.44 x 10^{-3} M). As a positive and negative control, the anionic polyelectrolytes PSS and PVS were used, respectively.

The presence of dispersed particles in aqueous medium was initially analyzed by turbidimetry in an Duetta spectrophotometer (Horiba, Japan). For that, the absorbance of 1 mL of each formulation was measured at a wavelength where none of the compounds (DOX and DNA) absorb (λ = 650 nm). Each sample was analyzed in triplicate at 25 °C.

The hydrodynamic diameter and zeta potential of the formulations were determined by DLS and laser Doppler anemometry (LDA), respectively, using a Zetasizer NanoZS (Malvern Instruments, UK) equipped with a standard λ = 633 nm laser as the incident beam. The formulations were diluted in Milli-Q water and loaded into a disposable folded capillary cuvette (DTS1070). The results were analyzed using the ZetaSizer v7.12 software. Each analysis was performed in triplicate at 25 °C.

The determination of the nanoparticle concentration was conducted in a NanoSight NS300 (Malvern Instruments, UK). The samples were diluted from 5 to 10 fold in Milli-Q water to achieve an optimum concentration range of

10^7 - 10^9 particles/mL. A minimum of five videos (one minute each one) of the particles moving under Brownian motion were captured. The videos were analyzed for size distribution and particle concentration using the built-in NTA v3.0 software (Malvern Instruments, UK) [51].

The morphological characterization was carried out in a scanning transmission electron microscope (STEM), model Inspect-50 (FEI, Holland). STEM images were obtained by sticking a droplet (20 µL) of the formulation to a copper grid (200 mesh, covered with Formvar) for 2 min, then removing the droplet with filter paper avoiding the paper touching the grid, then washing the grid twice with a droplet of a Milli-Q water for 1 min and removing the droplet with a filter paper. Subsequently, the sample was stained with a solution of 1 % (w/v) phosphotungstic acid by adding a droplet to the grid for 2 min and then removing with filter paper. The grid was dried at room temperature for at least 1 h prior to being analyzed [52].

2.5 Drug association, loading, and yield of DOX/DNA NPs

Drug association, loading, and yield were obtained as previously described [24]. The association efficiency of DOX in the NPs was determined by analyzing the ratio between the amount of drug associated in the formulation and the total initial drug (associated and non-associated). The drug loading (% w/w) was calculated by dividing the amount of drug associated in the formulation by the total weight of the NPs. The yield was calculated by dividing the total weight of NPs by the total weight of the components in the feed for each formulation (DOX + DNA). The drug content into the NPs was calculated indirectly by quantifying the free drug in the medium; the separation of NPs and free drug was done by using Vivaspin® 6 centrifugal tubes (MWCO 3.5 KDa, 5000 G x 40 min). The quantification of DOX was done by measuring the absorbance at 495 nm (Duetta spectrophotometer, Horiba Scientific, Japan), respectively. The standard curve of DOX was linear ($R^2 > 0.999$) in the range of concentrations between 1 x 10^{-5} M and 9 x 10^{-5} M (molar extinction coefficient was 9261.6 $M^{-1}cm^{-1}$). Finally, for the calculation of the total weight of the NPs, 1 mL of each formulation was lyophilized in glass vials, which were weighed before adding the formulation and after freeze-drying to assess the total solid mass (glass vials + formulation). The lyophilization procedure was done in the freeze-dryer equipment FreeZone 1 (Labconco, USA) using a high vacuum pump (50 mTorr) for 24 h.

2.6 In-vitro drug release studies

In-vitro release assays were carried out using conventional dialysis. 5 mL of DOX/DNA formulations were added in a dialysis bag (MWCO 10 kDa, ThermoScientific, USA). The dialysis system was immersed in 95 mL of Milli-Q water at pH 7 and kept at 37 °C, and 100 rpm in an orbital shaker (LSI-3016R, LabTech, Daihan LabTech, Kyonggi-Do, Korea). The experiment was carried out for 12 days; aliquots (500 µL) of the solution were withdrawn at certain time intervals and replaced with an equal volume of fresh Milli-Q water. The amount of released DOX was determined by measuring the absorbance of each aliquot by spectrophotometry (Duetta spectrophotometer, Horiba Scientific, Japan). To investigate the release mechanism, mathematical kinetics modelling was run using the program DDSolver [53]. The coefficient of determination (R^2), the Akaike information criteria (AIC), and the model selection criteria (MSC) parameters were considered for the model selection. Finally, the release data was fitted to zero order, first order, Higuchi and Korsmeyer-Peppas [23].

2.7 Viability assays (safety)

Non-cancerous HEK293 cells were seeded in 96-well plates at a density of 1 × 10^4 cells per well and incubated for 24 h in culture medium. Then, cells were treated for another 24 h with formulations (10 µL). Cell proliferation was evaluated removing DOX treatments and replacing with fresh culture medium containing 10% of tetrazolium compound of MTS® assay (CellTiter 96® Aqueous Non-Radioactive Cell Proliferation Assay), according to the manufacturer (Promega, Madison, WI) [54]. The soluble formazan produced by live cells was detected through its absorbance at 490 nm on a Multiscan Reader (Synergy-H4, Biotek) [55].

2.8 Stability assays of DOX/DNA NPs

The stability of the formulations was evaluated in terms of hydrodynamic diameter and zeta potential during 8 weeks using a ZetaSizer NanoZS.

3. RESULTS AND DISCUSSION

3.1. Exploring the interactions and binding of DOX and DNA

UV-vis spectroscopy is a simple and reliable method to study interactions and to determine the association of DNA with other molecules, including HALMW drugs [49]. DOX is a HALMW drug that contains an aromatic tetracyclic ring (anthracene) capable of establishing aromatic interactions [56, 57]. Also, it is well-known that DOX is capable to intercalate into de double-strand of DNA [53]. In our experiments, the concentration of DOX was kept constant at 3.5 × 10^{-5} M and DNA concentrations varied from 0 to 2.5 x 10^{-4} M. The effect of DNA on DOX absorbance is shown in **Figure 2A**.

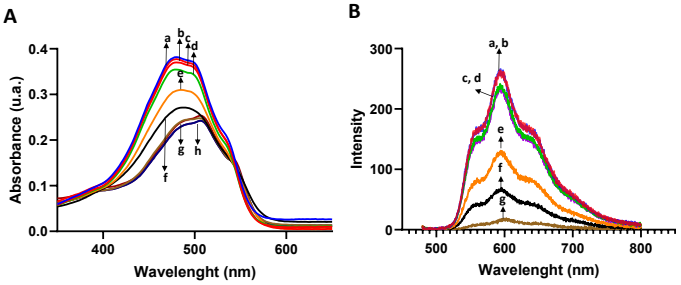

Figure 2. UV-visible (**A**) and fluorescence spectroscopy (**B**) of DOX (3.5 x 10^{-5} M) in the absence (**a**) and presence of DNA [1 x 10^{-6} M (**b**), 5 x 10^{-6} M (**c**), 1 x 10^{-5} M (**d**), 2.5 x 10^{-5} M (**e**), 5 x 10^{-5} M (**f**), 2 x 10^{-4} M (**g**), 2.5 x 10^{-4} M (**h**).

The results showed that the DOX absorption band (at λ = 495 nm) exhibited a bathochromic shift of up to 10 nm at a DNA concentration of 2.5 x 10^{-4} M, indicating a decrease in the $\pi \rightarrow \pi^*$ transition energy of the DOX chromophore. This shift was accompanied by a progresive decrease in the absorption band (hypochromic effect) as the DNA concentration increased. Hypocromicity is attributed to a reduction in the electronic transition probabilities ($\pi \rightarrow \pi^*$) of DOX, caused by the partial filling of its π^* orbital [45]. In addition, DOX becomes confined between the base pairs of DNA, which restricts its rotational and vibrational freedom. These constraints affect the orientation of the transition dipole moment, thereby influencing the intensity of the absorption band [58]. These combined bathochromic and hypochromic effects are characteristic of intercalation events. In our case, since we used double-strand DNA, the obtained results strongly refer to DOX intercalation [44, 58]. To determinate the intrinsic binding constant, the absorbance values at 495 nm as a function of DNA concentration (between 1 x 10^{-6} M to 2.5 x 10^{-5} M), were fitted to the Wolfe-Shimer equation (Equation 1, Materials and Methods). The calculated association constant (K_b) for the DOX-DNA complexes was 1.5 × 10^7 M^{-1}. This value is consistent with DNA association constants reported by other authors for DOX (e.g., K_b = 2.04 x 10^6 M^{-1} [54]; K_b = 4.53 x 10^5 M^{-1} [55]) and for other classic intercalating molecules as ethidium bromide with a K_b = 1 x 10^7 M^{-1} [56].

To further investigate the interaction mode between the DOX and DNA, fluorescence spectroscopy was employed. **Figure 2B** shows the emission spectra of DOX both in the absence and in the presence of varying amounts of DNA (up to 2 x 10^{-4} M). Our results show a concentration-dependent decrease in DOX emission intensity as DNA concentrations increases. This fluorescence quenching is considered as evidence to the formation of complexes through aromatic interactions [49]. In addition, the quenching process is quantitatively described by the Stern-Volmer equation (equation 3, material and methods). By analyzing the fitting of the experimental data to this equation, we determined the quenching constant (K_{SV}) of 6.28 x 10^4 M^{-1}. This value is in agreement with other authors (K_{SV} of 2.5 x 10^4 M^{-1} [59]).

The above results refer to a strong DOX association to DNA via intercalation upon mixing aqueous solutions. We hypothesize that, at selected experimental conditions, the attractive interactions could be enough for providing DNA-based NPs.

3.2 DOX/DNA NPs: Elaboration and characterization

To explore the possibility of obtaining DOX/DNA NPs, DOX and DNA were mixed varying the molar ratios ([DOX]/[DNA]) from 0.1 to 1.0. The DNA concentration was fixed (1.44 x 10^{-3} M), varying the DOX concentration (1.44 x 10^{-4} - 1.44 x 10^{-3} M). 500 µL of DOX were added to 500 µL of DNA (pH 7, room temperature) followed by 5 min of stirring. The obtained formulations were firstly analyzed by turbidimetry (λ = 650 nm). Significant increase in the absorption at 650 nm is indicative of the presence of colloidal system, presumably in the scale of nanometers [23-25]. For the DOX/DNA formulations, significant turbidity was observed at molar ratios between 0.5 and 0.6 (**Figure 3A**); beyond this molar ratio, precipitation occurs. Dynamic light scattering (DLS) analysis of selected formulations (DOX/DNA 0.5 and DOX/DNA 0.6) confirmed the presence of NPs with a hydrodynamic size between 118 - 220 nm and polydispersity (PdI) between 0.39 - 0.46. Laser Doppler anemometry determined a zeta potential of -26.3 to -27.7 mV and nanoparticle tracking analysis (NTA) showed a concentration of 8.41 x 10^{11} to 13.5 x 10^{11} particles/mL (**Figure 3B**) for these formulations. STEM results revealed that the particles were spheroidal (**Figure 3C**). As expected, formulations tested with the aromatic polyelecytrolyte PSS (tested as positive control) yielded highly turbid formulations, corresponding to NPs with size between 140 to 302 nm, PDI of 0.33 – 0.47 and zeta potential of -35.2 to -37.7 mV (**Figure 3B**). In contrast, no turbidity or nanoparticle formation was observed in the presence of the aliphatic polyelectrolyte PVS (tested as negative control, **Figure 3A**), thereby corroborating the critical role of the presence of aromatic groups in the polyelectrolyte to obtain NPs. It is important to highlight that the presence of aromatic rings and complementary charges (DOX being cationic and DNA anionic) allows for key non - covalent interactions, mainly aromatic - aromatic and electrostatic interactions. In this system, DOX intercalates between the base pairs of DNA, providing additional stability and enhancing the overall interaction strength of the complex [60]. At the same time, electrostatic interactions may contribute to the progressive neutralization of the negative charge on DNA, possibly promoting polymer chain collapse and the formation of aggregates, which could ultimately lead to the spontaneous formation of nanoparticles [23-25].

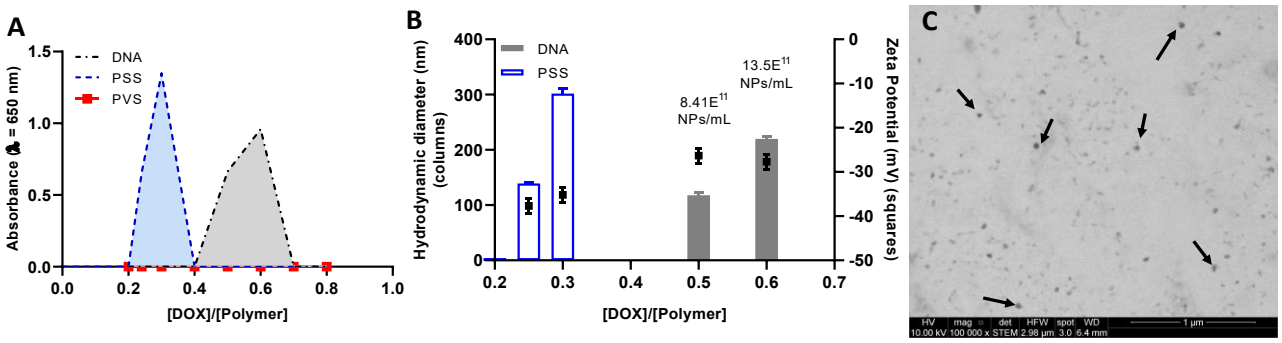

Figure 3.- Turbidimetry of DOX/polymer formulations at molar ratios between 0.1 and 1 (**A**). Hydrodynamic diameter (bars) and zeta potential (squares) of the DOX/polymer formulations at molar ratios between 0.2 and 0.7 (**B**). STEM micrograph of the DOX/DNA NPs at molar ratio 0.5 (**C**).

We also analyzed the association parameters for the selected DOX/DNA NPs. The results showed association efficiencies ranging from 66 to 80%, drug loading capacity of 41-57%, and yield of 67-85%. Notably, the drug loading capacity achieved is remarkable compared to other DOX-encapsulating nanosystems (nanoemulsions, liposomes). For instance, Jiang *et al.* [61] synthesized DOX nanoemulsions with a drug loading of 3.8%. Similarly, Alyane *et al* [62] encapsulated DOX into liposomes with a loading of 5%. The lower loading values obtained in these formulations are primarily attributed to less efficient interactions between DOX and the selected excipients, and to the use of a larger number of excipients. In contrast, for the formulations prepared using our methodology, DOX is a structural component of the nanoparticle, contributing to the formation/stabilization, and enabling high encapsulation parameters.

3.3 DOX/DNA NPs: In-vitro release, viability and stability

For the release assay, 5 mL of the DOX/DNA NPs (molar ratio 0.5) was subjected to dialysis at 37 °C and continuous agitation. **Figure 4A** shows the cumulative release profile of DOX over time. The obtained results evidenced a two-phase release process, demonstrating an initial burst release of 18% within the first 6 h. This event was followed by the ability of the nanoparticle to retain DOX, resulting in a cumulative release that did not exceed the 55% over 12 days. These results contrast with other nanosystems where DOX release exceeds ≈ 40% [61], ≈ 50-70% [63], and ≈ 70-80 % [21] within 6 h. To understand the release mechanism of our nanoformulations, we analyzed the fit of the experimental data to different models, including zero-order, first-order, Higuchi, and Korsmeyer-Peppas. The selected model was based on the coefficient of determination (R^2), the Akaike Information Criterion (AIC), and the Model Selection Criterion (MSC). The model that showed the best fit was identified as the one with the highest R^2, lowest AIC, and highest MSC values. The analysis showed that the Korsmeyer-Peppas model provided the best fit for the formulation (**Figure S1**, supplementary information). This model is characteristic of NPs comprising only two components, drug and polymer, mediated by aromatic interactions [23-25]. In these nanoparticle formulations, the release process is associated to a swelling mechanism, accompanying several structural changes including alterations in macromolecular conformation and chain mobility, changes in the extent of aggregate hydration, and variations in the size and distribution of swollen areas [23, 64-66]. Importantly, as evidenced in **Figure 4B**, the formulations remained stable for 8 weeks, which agrees with the slow drug release profile (**Figure 4A**), and afford good stability under storage and/or after reconstitution in aqueous medium.

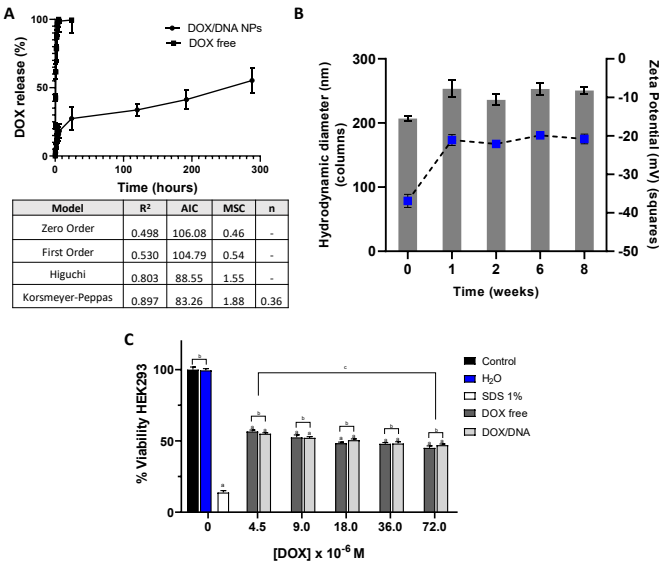

Model	R^2	AIC	MSC	n
Zero Order	0.498	106.08	0.46	-
First Order	0.530	104.79	0.54	-
Higuchi	0.803	88.55	1.55	-
Korsmeyer-Peppas	0.897	83.26	1.88	0.36

Figure 4.- In vitro release profile at pH 7.0 (37 °C) of DOX/DNA 0.5 NPs and their adjusment to various kinetic models (A). DOX/DNA NPs stability in time (B). Viability of non-cancerous cells line (HEK293) after treatment with DOX/DNA 0.5 NPs for 24 h (mean values ± SEM, n = 3, "a" indicates significant differences compared to the control ($p < 0.01$), "b" indicates non-significant differences ($p > 0.05$), "c" indicates significant differences between groups ($p < 0.01$). (C).

In terms of safety, as evidenced in **Figure 4C**, a dose dependent tendency was observed in the non-cancerous cell line (HEK293) for DOX and DOX/DNA NPs at the tested doses. These results suggest that the encapsulation process maintains the inherent cytotoxic profile of DOX without introducing additional toxicity to HEK293 cells. Such findings are consistent with previous studies reporting similar cytotoxic effects between free and encapsulated doxorubicin in non-cancerous cell lines [67], highlighting the potential of the encapsulation system to deliver doxorubicin without exacerbating off-target toxicity. DNA-based nanoparticles present significant advantages due to their biocompatibility and versatility as structural materials. However, it is important to acknowledge that the use of DNA may elicit immunological responses under certain conditions. For example, DNA nanoparticles can be recognized by components of the innate immune system, such as Toll-like receptor, which detects unmethylated CpG motifs, potentially triggering mild inflammatory responses [68, 69]. These effects depend on factors like dosage, delivery route, and nanoparticle design. Despite these considerations, the unique benefits of DNA as a building block for nanostructures make it a valuable material in nanomedicine. With careful design and optimization, potential immunogenicity and side effects can be minimized, allowing DNA-based nanoparticles acting as effective and safe platforms for therapeutic applications.

CONCLUSIONS

In this study, we successfully entrapped doxorubicin (DOX) within a DNA-based NPs, using DNA as a unique excipient. UV-vis and fluorescence spectroscopy studies confirmed the strong association between DOX and DNA. Subsequently, a simple methodology by mixing two aqueous solutions, enabled the creation of reproducible NPs with hydrodynamic diameters between 115-220 nm, polydispersity of 0.39-0.45, zeta potential of ~-27 mV and $8x10^{11}$ to $13x10^{11}$ NPs / mL. In addition, the obtained NPs exhibited DOX association efficiency of 66-80% and very high loading (40-60%). DOX/DNA NPs demonstrated a prolonged release (55% in 12 days), stability at storage (at least 8 weeks) and did not provide toxicity in non-cancerous cells. The NPs developed in this study represent an efficient and safe platform for DOX delivery that can be extrapolated to other antineoplastic drugs possessing similar physicochemical properties (hydrophilic, aromatic, and low-molecular-weight). In additon, other nucleotides based drugs proposed for cancer therapy could be combined with DOX (or similar drugs) in order to confer dual activity.

AUTHOR CONTRIBUTIONS

Conceptualization, M.G.V-S., A.F.G.Q., F.A.O-A., M.B., I.M-V.; methodology, M.G.V-S and E.E-B.; formal analysis, M.G.V-S, A.F.G.Q., F.A.O-A., M.B., I.M-V and E.E.-B; investigation, M.G.V-S and E.E-B.; resources, F.O-A., M.B, A.F.G.Q; data curation, M.G.V-S. and E.E.-B; writing original draft preparation, M.G.V-S., E.E-B, F.A.O-A; writing-review and editing, A.F.G.Q, F.A.O-A, M.B, I.M-V. and M.G.V-S.; supervision, F.A.O-A., A.F.G.Q, M.B. and I.M-V.; project administration, F.A.O-A, M.B, I.M-V. and M.G.V-S; funding acquisition, F.A.O-A, M.B, I.M-V. and M.G.V-S. All authors have read and agreed to the published version of the manuscript.

FUNDING

This work was supported by FONDECYT 3210549 (M.G.V-S), ANID/ACT240058 (F.A.O-A), FONDECYT 3240634 (E.E-B); FONDECYT 1241624 (F.A.O-A.), FONDECYT 1251598 (A.F.G.Q), FONDECYT 1250392 (I.M-V.), FONDECYT 1231276 (M.B.), FONDEQUIP EQM160157 (F.A.O-A), Fondo de Investigación Avanzada en Áreas Prioritarias (FONDAP) Grant 15130011 and Continuation grant 1523A0008 (A.F.G.Q., F.A.O-A).

INFORMED CONSENT STATEMENT

Not applicable.

CONFLICTS OF INTEREST

The authors declare no conflicts of interest.

ABBREVIATIONS

The following abbreviations are used in this manuscript:

DOX	Doxorubicin
DNA	Deoxyribonucleic acid
PSS	Poly(4-styrenesulfonate)
PVS	Poly(vinylsulfonate)
NPs	Nanoparticles
HLMW	Hydrophilic, aromatic, low molecular weight

REFERENCES

1. Bray, F., et al., *Global cancer statistics 2022: GLOBOCAN estimates of incidence and mortality worldwide for 36 cancers in 185 countries.* 2024. **74**(3): p. 229-263.
2. Nagai, H. and Y.H. Kim, *Cancer prevention from the perspective of global cancer burden patterns.* J Thorac Dis, 2017. **9**(3): p. 448-451.
3. ReFaey, K., et al., *Cancer Mortality Rates Increasing vs Cardiovascular Disease Mortality Decreasing in the World: Future Implications.* Mayo Clin Proc Innov Qual Outcomes, 2021. **5**(3): p. 645-653.
4. Rache, B., et al., *Transition towards cancer mortality predominance over cardiovascular disease mortality in Brazil, 2000–2019: a population-based study.* The Lancet Regional Health – Americas, 2024. **39**.
5. Xia, W. and M.W. King, *Advances in Targeted Delivery of Doxorubicin for Cancer Chemotherapy.* 2025. **12**(4): p. 430.
6. Melguizo, C., et al., *Enhanced antitumoral activity of doxorubicin against lung cancer cells using biodegradable poly(butylcyanoacrylate) nanoparticles.* Drug Des Devel Ther, 2015. **9**: p. 6433-44.
7. Sritharan, S. and N. Sivalingam, *A comprehensive review on time-tested anticancer drug doxorubicin.* Life Sci, 2021. **278**: p. 119527.
8. Methaneethorn, J., et al., *Population pharmacokinetics of doxorubicin: A systematic review.* Asia-Pacific Journal of Clinical Oncology, 2023. **19**(1): p. 9-26.
9. Sinha, S.J., et al., *Emerging Research and Future Directions on Doxorubicin: A Snapshot.* Asian Pac J Cancer Prev, 2025. **26**(1): p. 5-15.
10. Yu, L.-R. and V.G. Desai, *Doxorubicin Cardiotoxicity: Preclinical and Clinical Circulating Protein Markers*, in *Biomarkers in Toxicology*, V.B. Patel, V.R. Preedy, and R. Rajendram, Editors. 2023, Springer International Publishing: Cham. p. 677-703.
11. Lele, K.A., et al., *Targeting cardiotoxicity: the potential of Annona squamosa L. in doxorubicin therapy.* In Silico Pharmacology, 2025. **13**(1): p. 47.
12. Linders, A.N., et al., *A review of the pathophysiological mechanisms of doxorubicin-induced cardiotoxicity and aging.* npj Aging, 2024. **10**(1): p. 9.
13. Gautam, S., et al., *Recent doxorubicin-conjugates in cancer drug delivery: Exploring conjugation strategies for enhanced efficacy and reduced toxicity.* International Journal of Pharmaceutics, 2025. **675**: p. 125556.
14. Ghahremanloo, A., et al., *Reducing toxicity and enhancing efficacy of doxorubicin by liposomal doxorubicin and aprepitant in breast cancer.* Scientific Reports, 2025. **15**(1): p. 9798.
15. Bisht, A., et al., *A comprehensive review on doxorubicin: mechanisms, toxicity, clinical trials, combination therapies and nanoformulations in breast cancer.* Drug Delivery and Translational Research, 2025. **15**(1): p. 102-133.
16. Dehghani, B., M. Mirzaei, and A. Lohrasbi-Nejad, *Characterization of Thermoresponsive Poly(N-vinylcaprolactam) Polymer Containing Doxorubicin-Loaded Niosomes: Synthesis, Structural Properties, and Anticancer Efficacy.* Journal of Pharmaceutical Innovation, 2025. **20**(1): p. 7.
17. Zang, C., et al., *Hydrogel-based platforms for site-specific doxorubicin release in cancer therapy.* Journal of Translational Medicine, 2024. **22**(1): p. 879.
18. Zhao, H., et al., *Doxorubicin prodrug-based nanomedicines for the treatment of cancer.* Eur J Med Chem, 2023. **258**: p. 115612.
19. Rodríguez, F., et al., *Nano-Based Approved Pharmaceuticals for Cancer Treatment: Present and Future Challenges.* Biomolecules, 2022. **12**(6).
20. Fatima, W., et al., *Controlled release of doxorubicin from gelatin-based nanoparticles: theoretical and experimental approach.* Materials Advances, 2024. **5**(6): p. 2347-2358.
21. Norouzi, M., et al., *Doxorubicin-loaded iron oxide nanoparticles for glioblastoma therapy: a combinational approach for enhanced delivery of nanoparticles.* Scientific Reports, 2020. **10**(1): p. 11292.
22. Misiak, P., et al., *Doxorubicin-loaded polymeric nanoparticles containing ketoester-based block and cholesterol moiety as specific vehicles to fight estrogen-dependent breast cancer.* Cancer Nanotechnology, 2023. **14**(1): p. 23.

23. Villamizar-Sarmiento, M.G., et al., *The key role of the drug self-aggregation ability to obtain optimal nanocarriers based on aromatic-aromatic drug-polymer interactions.* European Journal of Pharmaceutics and Biopharmaceutics, 2021. **166**: p. 19-29.
24. Villamizar-Sarmiento, M.G., et al., *A New Methodology to Create Polymeric Nanocarriers Containing Hydrophilic Low Molecular-Weight Drugs: A Green Strategy Providing a Very High Drug Loading.* Molecular Pharmaceutics, 2019. **16**(7): p. 2892-2901.
25. Villamizar-Sarmiento, M.G., et al., *Colloidal nanomedicines with prolonged release of chloroquine based on interactions with aromatic polymers after mixing two liquids: from in silico simulation of nanoparticle formation to efficient in-bench scale up.* Journal of Molecular Liquids, 2024. **395**: p. 123906.
26. Hu, Q., et al., *DNA Nanotechnology-Enabled Drug Delivery Systems.* Chem Rev, 2019. **119**(10): p. 6459-6506.
27. Chen, T., et al., *DNA Nanotechnology for Cancer Diagnosis and Therapy.* Int J Mol Sci, 2018. **19**(6).
28. Kumar, V., et al., *DNA Nanotechnology for Cancer Therapy.* Theranostics, 2016. **6**(5): p. 710-725.
29. Zhang, Q., et al., *DNA origami as an in vivo drug delivery vehicle for cancer therapy.* ACS Nano, 2014. **8**(7): p. 6633-43.
30. Zhao, Y.-X., et al., *DNA Origami Delivery System for Cancer Therapy with Tunable Release Properties.* ACS Nano, 2012. **6**(10): p. 8684-8691.
31. Li, J., et al., *Functional nucleic acid-based hydrogels for bioanalytical and biomedical applications.* Chemical Society Reviews, 2016. **45**(5): p. 1410-1431.
32. Hurst, S.J., A.K. Lytton-Jean, and C.A. Mirkin, *Maximizing DNA loading on a range of gold nanoparticle sizes.* Anal Chem, 2006. **78**(24): p. 8313-8.
33. Khuu, A., et al., *Clinical Applications of Antisense Oligonucleotides in Cancer: A Focus on Glioblastoma.* 2024. **13**(22): p. 1869.
34. Xiong, H., R.N. Veedu, and S.D. Diermeier, *Recent Advances in Oligonucleotide Therapeutics in Oncology.* Int J Mol Sci, 2021. **22**(7).
35. Oprea, M. and M. Ionita, *Antisense oligonucleotides-based approaches for the treatment of multiple myeloma.* International Journal of Biological Macromolecules, 2025. **291**: p. 139186.
36. Zhang, J., et al., *A Comprehensive Review of Small Interfering RNAs (siRNAs): Mechanism, Therapeutic Targets, and Delivery Strategies for Cancer Therapy.* Int J Nanomedicine, 2023. **18**: p. 7605-7635.
37. Kalaimani, K., et al., *Recent advancements in small interfering RNA based therapeutic approach on breast cancer.* European Journal of Pharmacology, 2024. **981**: p. 176877.
38. Liu, C., et al., *mRNA-based cancer therapeutics.* Nature Reviews Cancer, 2023. **23**(8): p. 526-543.
39. Kong, B., et al., *mRNA: A promising platform for cancer immunotherapy.* Advanced Drug Delivery Reviews, 2023. **199**: p. 114993.
40. Afzal, A., et al., *Current Trends in Messenger RNA Technology for Cancer Therapeutics.* Biomater Res, 2025. **29**: p. 0178.
41. Menon, A., et al., *miRNA: A Promising Therapeutic Target in Cancer.* Int J Mol Sci, 2022. **23**(19).
42. Szczepanek, J., M. Skorupa, and A. Tretyn, *MicroRNA as a Potential Therapeutic Molecule in Cancer.* Cells, 2022. **11**(6).
43. Wang, Z., et al., *miRNA interplay: Mechanisms and therapeutic interventions in cancer.* MedComm – Oncology, 2024. **3**(4): p. e93.
44. Kashanian, S., et al., *Multi-spectroscopic DNA interaction studies of sunset yellow food additive.* Mol Biol Rep, 2012. **39**(12): p. 10045-51.
45. Wolfe, A., G.H. Shimer, Jr., and T. Meehan, *Polycyclic aromatic hydrocarbons physically intercalate into duplex regions of denatured DNA.* Biochemistry, 1987. **26**(20): p. 6392-6.
46. Kamat, V., et al., *Emphasized DFT, DNA binding, and electrochemical studies of hybrid 1,3,4-thiadiazole-linked chalcone confined via a sulfur bridge.* Journal of Chemical Sciences, 2024. **136**(2): p. 31.
47. Chauhan, M. and F. Arjmand, *Chiral and achiral macrocyclic copper(II) complexes: Synthesis, characterization, and comparative binding studies with calf-thymus DNA.* Chem Biodivers, 2006. **3**(6): p. 660-76.
48. Elsayed, S.A., et al., *Palladium(ii), platinum(ii), and silver(i) complexes with 3-acetylcoumarin benzoylhydrazone Schiff base: Synthesis, characterization, biomolecular interactions, cytotoxic activity, and computational studies.* RSC Advances, 2024. **14**(27): p. 19512-19527.
49. Sirajuddin, M., S. Ali, and A. Badshah, *Drug–DNA interactions and their study by UV–Visible, fluorescence spectroscopies and cyclic voltametry.* Journal of Photochemistry and Photobiology B: Biology, 2013. **124**: p. 1-19.
50. Shahabadi, N., S. Mohammadi, and R. Alizadeh, *DNA Interaction Studies of a New Platinum(II) Complex Containing Different Aromatic Dinitrogen Ligands.* Bioinorg Chem Appl, 2011. **2011**: p. 429241.
51. Villamizar-Sarmiento, M.G., et al., *Ionic Nanocomplexes of Hyaluronic Acid and Polyarginine to Form Solid Materials: A Green Methodology to Obtain Sponges with Biomedical Potential.* 2019. **9**(7): p. 944.
52. Inostroza-Riquelme, M., et al., *Encapsulation of Gold Nanostructures and Oil-in-Water Nanocarriers in Microgels with Biomedical Potential.* 2018. **23**(5): p. 1208.
53. Zhang, Y., et al., *DDSolver: an add-in program for modeling and comparison of drug dissolution profiles.* Aaps j, 2010. **12**(3): p. 263-71.
54. Zárate, A.M., et al., *A New Smoothened Antagonist Bearing the Purine Scaffold Shows Antitumour Activity In Vitro and In Vivo.* 2021. **22**(16): p. 8372.
55. Guerrero, S., et al., *Curcumin-loaded nanoemulsion: a new safe and effective formulation to prevent tumor reincidence and metastasis.* Nanoscale, 2018. **10**(47): p. 22612-22622.
56. Yaghoubi, A. and A. Ramazani, *Anticancer DOX delivery system based on CNTs: Functionalization, targeting and novel technologies.* J Control Release, 2020. **327**: p. 198-224.
57. Zarzhitsky, S. and H. Rapaport, *The interactions between doxorubicin and amphiphilic and acidic β-sheet peptides towards drug delivery hydrogels.* Journal of Colloid and Interface Science, 2011. **360**(2): p. 525-531.
58. Jawad, B., et al., *Molecular mechanism and binding free energy of doxorubicin intercalation in DNA.* Physical Chemistry Chemical Physics, 2019. **21**(7): p. 3877-3893.
59. Agudelo, D., et al., *Review on the binding of anticancer drug doxorubicin with DNA and tRNA: Structural models and antitumor activity.* Journal of Photochemistry and Photobiology B: Biology, 2016. **158**: p. 274-279.
60. Ijäs, H., et al., *Unraveling the interaction between doxorubicin and DNA origami nanostructures for customizable chemotherapeutic drug release.* Nucleic Acids Res, 2021. **49**(6): p. 3048-3062.
61. Jiang, S.-P., et al., *Preparation and characteristics of lipid nanoemulsion formulations loaded with doxorubicin.* International Journal of Nanomedicine, 2013. **8**: p. 3141-50.
62. Alyane, M., G. Barratt, and M. Lahouel, *Remote loading of doxorubicin into liposomes by transmembrane pH gradient to reduce toxicity toward H9c2 cells.* Saudi Pharm J, 2016. **24**(2): p. 165-75.
63. Assali, M., N. Jaradat, and L. Maqboul, *The Formation of Self-Assembled Nanoparticles Loaded with Doxorubicin and d-Limonene for Cancer Therapy.* ACS Omega, 2022. **7**(46): p. 42096-42104.
64. Ahmed, L., et al., *Study the Using of Nanoparticles as Drug Delivery System Based on Mathematical Models for Controlled Release.* 2019. **8**: p. 52-56.
65. Heredia, N.S., et al., *Comparative statistical analysis of the release kinetics models for nanoprecipitated drug delivery systems based on poly(lactic-co-glycolic acid).* PLoS One, 2022. **17**(3): p. e0264825.
66. Contri, R.V., et al., *Drug Release from Pharmaceutical Nanocarriers*, in *The ADME Encyclopedia: A Comprehensive Guide on Biopharmacy and Pharmacokinetics*, A. Talevi, Editor. 2022, Springer International Publishing: Cham. p. 419-428.
67. Zhang, B., et al., *The anti-tumor and renoprotection study of E-[c(RGDfK)2]/folic acid co-modified nanostructured lipid carrier loaded with doxorubicin hydrochloride/salvianolic acid A.* Journal of Nanobiotechnology, 2022. **20**(1): p. 425.
68. Arancibia, S.A., et al., *Toll-like receptors are key participants in innate immune responses.* Biol Res, 2007. **40**(2): p. 97-112.
69. Kumagai, Y., O. Takeuchi, and S. Akira, *TLR9 as a key receptor for the recognition of DNA.* Advanced Drug Delivery Reviews, 2008. **60**(7): p. 795-804.